



High macrophage activities are associated with advanced periductal fibrosis in chronic *Opisthorchis viverrini* infection

Journal:	<i>Parasite Immunology</i>
Manuscript ID	Draft
Manuscript Type:	Original Paper
Date Submitted by the Author:	n/a
Complete List of Authors:	Salao, Kanin; Khon Kaen University Faculty of Medicine, Microbiology Watakulsin, Krongkarn; Khon Kaen University Faculty of Medicine, Microbiology Mairiang, Eimorn; Khon Kaen University Faculty of Medicine, Radiology Suttiprapa, Sutas; Khon Kaen University Faculty of Medicine, Academic Affairs Tangkawattana, Sirikachorn; Khon Kaen University Faculty of Veterinary Medicine, Pathobiology Edwards, Steven; University of Liverpool School of Life Sciences, Integrative Biology Sripa, Banchob; Faculty of Medicine, Khon Kaen University, Department of Pathology
Key Words:	Macrophage < Cell, Peripheral blood mononuclear cells < Cell, Human < Host species, Innate immunity < Immunological terms, <i>Opisthorchis viverrini</i> < Parasite, Flow cytometry < Tools and techniques

High macrophage activities are associated with advanced periductal fibrosis in chronic *Opisthorchis viverrini* infection

Running title: Innate immunity in opisthorchiasis

Kanin Salao^{1,7}, Krongkarn Watakulsin^{1,7}, Eimorn Mairiang², Sutas Suttiaprapa^{3,7}, Sirikachorn Tangkawattan^{4,7}, Steven W. Edwards⁵, Banchob Sripa^{6,7*}

¹Department of Microbiology, Faculty of Medicine, Khon Kaen University, Khon Kaen 40002, THAILAND, Email: kaninsa@kku.ac.th

¹Department of Microbiology, Faculty of Medicine, Khon Kaen University, Khon Kaen 40002, THAILAND, Email: Watakarn@kkumail.com

²Department of Radiology, Faculty of Medicine, Khon Kaen University, Khon Kaen 40002, THAILAND, Email: eimmai@kku.ac.th

³Tropical Medicine Graduate Program (International Program), Academic Affairs,, Faculty of Medicine, Khon Kaen University, Khon Kaen 40002, THAILAND, Email: sutasu@kku.ac.th

⁴Department of Pathobiology, Faculty of Veterinary Medicine, Khon Kaen University, Khon Kaen 40002, THAILAND, Email: sirikach@kku.ac.th

⁵ Institute of Integrative Biology, Faculty of Health and Life Sciences, University of Liverpool, Liverpool L69 7ZB, UK, Email: S.W.Edwards@liverpool.ac.uk

⁶Department of Pathology, Faculty of Medicine, Khon Kaen University, Khon Kaen 40002, THAILAND, Email: banchob@kku.ac.th

⁷ WHO Collaborating Centre for Research and Control of Opisthorchiasis (Southeast Asian Liver Fluke Disease), Tropical Disease Research Center, Faculty of Medicine, Khon Kaen University, Khon Kaen 40002, THAILAND

*** Corresponding author:** Dr.Banchob Sripa, Tropical Disease Research Center (TDRC), Department of Pathology, Faculty of Medicine, Khon Kaen University, Khon Kaen 40002,

28 Thailand. Tel: 66-43-363113, Fax: 66-43-204359, E-mail: banchob@kku.ac.th

29

1
2
3
4
5
6
7
8
9
10
11
12
13
14
15
16
17
18
19
20
21
22
23
24
25
26
27
28
29
30
31
32
33
34
35
36
37
38
39
40
41
42
43
44
45
46
47
48
49
50
51
52
53
54
55
56
57
58
59
60

Abstract

Liver fluke infection caused by *Opisthorchis viverrini* induces several hepatobiliary conditions including advanced periductal fibrosis (APF) and cholangiocarcinoma (CCA), but >25% of the infected population develops APF and 1% develop CCA. The innate immune response is the first line of defense, and macrophages are critical regulators of fibrosis. We hypothesized that macrophages from infected individuals have different capacities to either promote or suppress periductal fibrosis. We compared phagocytic activities of macrophages of healthy individuals and *O. viverrini*-infected individuals \pm APF, and found that macrophages from infected individuals with APF ingested significantly higher numbers of beads compared with healthy controls and *O. viverrini*-infected individuals without APF. To further investigate proteolytic activity, we monitored real-time phagosomal proteolysis of beads conjugated to DQ BODIPY-BSA using live-cell imaging. We show that macrophages from *O. viverrini*-infected individuals with APF also have elevated phagosomal proteolysis activity, which is consistent with their increased phagocytic activity. Additionally, stimulated ROS production by blood monocytes was higher in individuals with APF compared with healthy controls and infected individuals without APF. These results suggest that during *O. viverrini* infection, macrophages with high phagocytic and proteolytic activities together with elevated ROS production, are the phenotypes that can promote tissue damage, which results in periductal fibrosis.

Keywords: *Opisthorchis viverrini*; Innate immunity; Peripheral blood mononuclear cells, Macrophages; Human; Flow cytometry

52

53 1. INTRODUCTION

54 *Opisthorchis viverrini* infection is endemic in the Lower Mekong regions of Southeast Asia,
55 including Thailand, with approximately 8 million people infected, especially in the northeast of
56 Thailand where consumption of raw freshwater fishes harboring the infective stage of the parasite
57 is common (1). Infection can cause several disease manifestations of the bile duct including
58 cholangitis, cholelithiasis, advanced periductal fibrosis (APF) and the most severe complication,
59 cholangiocarcinoma (CCA) (2-6). APF provides the basis for malignant transformation to CCA.
60 Fibrosis occurs when tissues are damaged and normal wound healing responses persist or become
61 dysregulated (7), usually in response to repetitive tissue injury (8) such as chronic *O. viverrini*
62 infection (5). Repeated tissue damage results from a combination of factors induced by *O.*
63 *viverrini* such as 1) physical damage induced by feeding, 2) release of products such as reactive
64 oxygen species from innate immune cells, 3) and *O. viverrini*-induced host inflammation through
65 both innate and adaptive immunity (9). The latter mechanism, which involves host immune
66 responses, is well supported by several findings from our group and others, which have
67 confirmed that chronic *O. viverrini* infection promotes adaptive proinflammatory responses (10,
68 11), i.e. IL-6 production (11). However, to date, far less is known about *O. viverrini* effects on
69 innate immunity.

70 Macrophages provide defense in innate immunity and these innate immune cells are
71 among the earliest infiltrating cells after acute *O. viverrini* infection (9). Apart from host defense,
72 macrophages also play a pivotal role in tissue homeostasis and wound repair. In chronic *O.*
73 *viverrini* infection that usually leads to persistent inflammation, macrophages produce large

1
2
3
4 74 amounts of mediators that are potentially toxic to the parasites but these may also cause bystander
5
6 75 damage to surrounding host tissues. To compensate for this injury, a small subset of macrophages
7
8
9 76 induce tissue repair, which results in the formation of fibrosis or fibrogenesis (12).
10

11 77 We hypothesized that different rates of development of APF may be due to the
12
13 78 consequence of different levels of innate immune responses that vary among individuals. As
14
15 79 macrophages are part of the innate immune system and critical regulators of fibrosis (13), we
16
17 80 sought to determine if *O. viverrini*-infected individuals with APF possess active innate immune
18
19 81 responses (e.g. phagocytic, proteolytic activities and ROS production), and hence have a higher
20
21 82 risk of developing APF compared with individuals without APF. Unraveling this association
22
23 83 should take us a step closer toward identifying a high-risk group and possibly providing data for
24
25 84 early and effective diagnosis or primary prevention of APF and CCA.
26
27
28
29

30 85

31
32 86 **2. MATERIALS AND METHODS**
33

34 87 **2.1 Sample recruitment**
35

36 88 The current study is an analysis of baseline data collected from a community-based, case-control
37
38 89 study of risk factors associated with the development of APF using high resolution
39
40 90 ultrasonography, as previously described (14), from ten villages including Bankae, Banbor,
41
42 91 Nongtu, Nonmakum, Saadsomsri, Jikngam, Songplui, Nhonkho, Huahad, and Somhong in
43
44 92 Kalasin province (Thailand). Overall, 332 individuals aged between 20 and 60 years old were
45
46 93 recruited into this study. The control group consisted of 102 *O. viverrini*-infected individuals (60
47
48 94 males, 42 females) without APF (APF-), while the case group consisted of 104 *O. viverrini*-
49
50 95 infected individuals (58 males and 46 females) with APF (APF +). A group of healthy donors
51
52
53
54
55
56
57
58
59
60

consisted of 126 *O. viverrini*-negative participants (68 males and 58 females) (Ov-). Written informed consents were obtained from all participants. This study complied with the standard good clinical practice (GCP) guideline and was approved by the Ethics Committee of Khon Kaen University, Khon Kaen, Thailand, reference number HE591185 and HE480528.

2.2 Sample size calculation

A statistical power analysis was performed for sample size estimation based on data from a published study (14). The effect size in this study was 0.5, which is considered medium by Cohen's (1988) criteria. With an $\alpha = 0.05$ and power = 0.80, the projected sample size needed for this effect size (G*Power 3.1 analysis) is approximately $n = 51$ per group for the simplest between-group comparison. Thus, our sample size of >100 per group was more than adequate for the main objective of this study.

2.3 Ultrasonography

A detailed description of the ultrasonography methods used in this study can be found in previous publications (14, 15). Using a mobile, high-resolution ultrasound (US) machine (GE model LOGIQ Book XP, GE healthcare, WI), hepatobiliary abnormalities including portal vein radical echoes, echoes in liver parenchyma, indistinct gallbladder wall, gallbladder size, sludge and suspected CCA were graded and recorded. Individuals were classified as having “non-advanced periductal fibrosis” or “APF-” if the US grade was 0 or 1, and “advanced periductal fibrosis” or “APF+” if the US grade was 2 or 3. Individuals with alcoholic liver disease, which is seen as fatty liver by US examination, were excluded. Individuals with marked hepatic fibrosis not

related to *O. viverrini* infection (e.g., cirrhosis from HBV or HCV) were also excluded from this study.

2.4 Blood collection

A total of 20 mL of venous blood collected from the participants by venipuncture, 8 mL of which was collected in sodium heparin sprayed coated tubes (cat# 367871, Becton Dickinson, NJ) and used for monocyte isolation.

2.5 Monocyte isolation for subsequent macrophage generation

The monocyte-derived macrophages (MDMs) used in this study were from peripheral blood monocytes isolated using a double gradient centrifugation method (16). Briefly, 8 mL of blood was overlaid on top of 6 mL of Ficoll solution (1.077 g/ml)(cat# 17-1440-02, GE Healthcare Life Sciences, Singapore) in a 15 mL Falcon tube (cat# 352097, Becton Dickinson, NJ) before centrifuging at 400x g without braking for 45 min at room temperature. The white band of peripheral blood mononuclear cells (PBMCs) at the interface was collected and washed 3 times with PBS and resuspended in 9 mL of RPMI-1640 medium (Cat #11875-093, Thermo Fisher Scientific, CA). For the second density gradient, 9 mL of the RPMI-resuspended PBMCs were placed on top of 6 mL of Percoll solution (1.131 g/mL) (cat# 28-9038-33, GE Healthcare Life Sciences, Singapore) in a 15-mL Falcon tube and centrifuged at 550x g without braking for 45 min at room temperature. The band of monocytes at the interface between the two phases was collected and washed 3 times with PBS. Monocytes were allowed to differentiate into macrophages by culturing in RPMI medium supplemented with 10% autologous serum on a 35-

mm petri dish (cat# CLS430165, Corning Inc., NY) for 7 days. The MDMs were then cultured in complete medium (RPMI medium containing 100 µg/mL streptomycin (Cat #15140-122, Thermo Fisher Scientific, CA), 2 mM L-glutamine (Cat #25030-081, Thermo Fisher Scientific, CA), 50 µM 2-mecaptoethanol, and 10% heat-inactivated fetal calf serum (Cat #14190-250, Thermo Fisher Scientific, CA).

2.7 Preparation of Alexa Fluor 594 dye and bodipy-BSA conjugated silica beads

The preparation of silica beads was adapted from the protocol described by Yates and Russell (17). Briefly, 3.0-µm carboxylate-modified silica particles (Cat #PSi-3.0COOH, Kisker Products for Biotechnologies, Germany) were conjugated with Alexa Fluor 594 Succinimidyl Esters (mixed isomers) (Alexa594-SE, Cat #A20004, Thermo Fisher Scientific, CA) or DQ green BODIPY bovine serum albumin (DQ-BODIPY BSA, Cat #D-12050, Thermo Fisher Scientific, CA). For opsonization, 0.5 mL of silica beads (14 mg/mL) was mixed with 0.5 mL purified goat-IgG (5 µg/mL) (Cat # I9140, Sigma-Aldrich, MO) and incubated at 37°C in 5% CO₂ for 30 min. The opsonized silica beads were then washed, and resuspended in PBS at a concentration of 1 mg/mL.

2.8 Synchronized phagocytosis

MDMs that adhered to a 35-mm petri dish were washed 3 times with PBS and resuspended in complete medium and then placed on ice for 10 min. Five µL (2x10⁶ particles/mL) silica beads conjugated with red Alexa Fluor 594 fluorescent dye were added to the petri dish containing adhered MDMs and mixed gently. The MDMs were then incubated on ice for a further 10 min to

1
2
3
4
5
6
7
8
9
10
11
12
13
14
15
16
17
18
19
20
21
22
23
24
25
26
27
28
29
30
31
32
33
34
35
36
37
38
39
40
41
42
43
44
45
46
47
48
49
50
51
52
53
54
55
56
57
58
59
60

allow the beads to attach to the cell surface. Synchronised phagocytosis was then triggered by warming the dish to 37 °C.

2.9 Rate of Phagocytosis

After 60 min of synchronized phagocytosis of the beads by the MDMs at 37°C in a 5% CO₂ incubator, phagocytosis was stopped by 3 washes with PBS before adding 2 mL of 4% paraformaldehyde (Cat # P6148, Sigma-Aldrich, MO) and incubated at room temperature for 10 min for fixation. The fixed MDMs were then washed 3 times with PBS. Randomized images of a total of 100 images were captured using scanning modes for red Alexa Fluor 594 fluorescent dye (excitation 490 nm, emission 594 nm) using BioStation IM/IM-Q software version 2.21 available from BioStation IM-Q Time Lapse Imaging System (Nikon, Japan). Images were acquired using a x40 objective with randomized automated acquisition following the manufacturer’s instructions. The phagocytosed beads were manually counted by an investigator blinded to the group assignment.

2.10 Rate of Proteolysis

MDMs that adhered to the petri dish after undergoing synchronized phagocytosis were placed into a 37 °C chamber containing 5% CO₂ on BioStation IM. The fluorescence intensities of green reporter DQ BODIPY dye (excitation 490 nm, emission 525 nm) were acquired in 60 sec intervals for 60 min. Approximately 100 cells were analyzed per sample. The fluorescence intensity was measured using an ImageJ (64-bit) software (NIH, imagej.nih.gov/ij/download/)

and plotted against time using Prism 6 (GraphPad Software Inc., CA) for ratiometric data analysis of intraphagosomal proteolysis.

2.11 Measurement of ROS production

50 μ l of whole blood was incubated \pm GM-CSF (5 ng/mL) in a total volume of 100 μ l in phosphate-buffered saline. After 30 min incubation at 37°C, samples were treated with 5 μ M dihydrorhodamine 123 followed by addition of either 1 μ M fMet-Leu-Phe or 0.1 μ g/mL PMA for a further 5- or 15 min, respectively at 37°C. Flow cytometry was used to measure the production of ROS.

2.12 Statistical analysis

All data were expressed as the mean \pm SEM. Statistical comparisons were performed using the *t* test between groups. When serial measurements were taken over time, groups were compared using two-way repeated-measures ANOVA with Bonferroni correction for multiple comparisons. A *P* value <0.05 was considered statistically significant. All data were analyzed using GraphPad Prism 6.0 statistical software.

3. RESULTS

3.1 MDMs from *O. viverrini*-infected individuals with APF had high phagocytic activity.

MDMs from *O. viverrini*-infected individuals with APF phagocytosed more beads per cell than MDMs from healthy controls (Figures 1, A-D: 3.50 ± 0.09 vs 1.58 ± 0.87 ; $n=102$ /group with >100 cells analyzed per sample, $p=0.01$, unpaired *t* test) and *O. viverrini*-infected individuals

1
2
3
4 205 without APF (Figures 1, A-D: 3.50 ± 0.09 vs 1.48 ± 0.05 ; n=102/group with >100 cells analyzed
5
6 206 per patient, $p<0.001$, unpaired t test). We then calculated the percentage of macrophages that
7
8 207 phagocytosed the beads and found that the percentage of phagocytic cells was increased in
9
10 208 individuals with OV infection and increased further in APF+ individuals (Figure 1E). These data
11
12 209 provided the first indication of a possible association between macrophages with high phagocytic
13
14 210 activity and the presence of APF in chronic *O. viverrini* infection.
15
16
17
18 211

19
20 212 **3.2 MDMs from *O. viverrini*-infected individuals with APF had elevated phagosomal**
21
22 **proteolysis.**
23
24

25 214 We then measured the rate of intraphagosomal proteolysis of individual ingested beads, as the
26
27 215 rate of increased fluorescence of individual particles (increased fluorescence per ingested bead)
28
29 216 by fluorescence imaging microscopy. The rate of proteolysis of BSA protein after phagocytosis
30
31 217 (measured by BODIPY fluorescence intensity) by MDMs from *O. viverrini*-infected individuals
32
33 218 with APF (Figure 2C) was greater than that from non-APF individuals (Figure 2B) and healthy
34
35 219 controls (Figure 2A) at 30 min and 60 min after phagocytosis. The time course of BSA
36
37 220 proteolysis clearly indicated that MDMs from patients with *O. viverrini*-induced APF proteolysed
38
39 221 BSA faster than MDMs from the healthy controls (Figure 2D, n=102/group with 10-15 individual
40
41 222 beads measured for each sample, $p<0.001$, two-way repeated-measures ANOVA) and *O.*
42
43 223 *viverrini*-infected individuals without APF (Figure 2D, $p<0.001$, two-way repeated-measures
44
45 224 ANOVA).
46
47
48
49

50 225
51
52
53
54
55
56
57
58
59
60

3.3 ROS production is elevated in monocytes from *O. viverrini*-infected individuals with APF.

Because macrophages used in previous two experiments are derived from peripheral blood monocytes, we then measured the production of ROS from circulating monocytes in these three cohorts. We found that there were no differences between groups if the cells in unprimed cells regardless of the stimulants. For example, there were no differences in ROS production in GM-CSF primed or unprimed cells when stimulated by the protein kinase C activator, PMA (data not shown). However, significant differences in ROS production were observed in response to the peptide, fMet-Leu-Phe which activates receptor-mediated stimulation of ROS, particularly after exposure to priming agents. In the absence of the priming agent, GM-CSF, there were no differences in ROS production between the three cohorts and fMet-Leu-Phe did not activate ROS in the absence of GM-CSF (Figure 3A-C). However, monocytes from *O. viverrini*-infected individuals with APF produced significantly more ROS than healthy control monocytes and monocytes from *O. viverrini*-infected individuals without APF (Figure 3D). These data suggest that circulating monocytes from APF+ individual are capable of generated higher levels of ROS after priming and stimulation.

4. DISCUSSION

Liver fluke infection has been widely known for more than two decades as a major cause of several hepatobiliary diseases including APF (4). The immunopathogenesis of APF is well described and it is partly induced by host adaptive immune responses through interaction of several immune cells (9) such as T cells (18), B cells (18), cytokines (11) and reactive oxygen

1
2
3
4 248 species (19). However, far less is known about the role of host innate immune responses on APF
5
6 249 generation. Our studies demonstrate for the first time that MDMs from *O. viverrini*-infected
7
8 250 individuals who have APF have high phagocytosis (Figures 1) and high proteolysis activity
9
10 251 (Figure 2) when compared with both non-*O. viverrini*-infected controls and *O. viverrini*-infected
11
12 252 individuals without APF. Furthermore, circulating monocytes from infected individuals with APF
13
14 253 have elevated ability to generate ROS, compared to infected individuals without APF or healthy
15
16 254 controls. This suggests that the presence of APF may associate with the pro-inflammatory
17
18 255 phenotype of MDMs, consistent with several findings from our group and others (11, 14).
19
20
21
22

23 256 Phagocytosis is one of several ways for uptake of antigen by macrophages (20). This
24
25 257 process involves the vesicular internalization of solid insoluble particles and can subsequently
26
27 258 activate NF- κ B signal transduction to produce pro-inflammatory cytokines and antimicrobial
28
29 259 peptides (21). These pro-inflammatory products are toxic to invading pathogens, but could also
30
31 260 damage host tissues when deregulated, especially in chronic infection/inflammation. Thus,
32
33 261 enhanced phagocytosis found in MDMs from APF+ individuals could result in an excessive
34
35 262 production of pro-inflammatory mediators such as reactive oxygen species. Indeed, we measured
36
37 263 enhanced ROS production by monocytes in whole blood and found that this was significantly
38
39 264 elevated in infected individuals with APF. Reactive oxygen species could damage host tissues
40
41 265 surrounding the bile ducts, which in turn, undergo repair processes, which result in the
42
43 266 development of fibrosis (22). In support of this hypothesis, a previous study showed that a subset
44
45 267 of MDMs promotes fibrogenesis after chronic *O. viverrini*-induced tissue damage (23).
46
47
48
49

50 268 Another possible mechanism by which pro-inflammatory MDMs could lead to more
51
52 269 advanced fibrosis is by elevated proteolytic activity. Proteolysis activity is tightly regulated by a
53
54
55
56
57
58
59
60

number of protease enzymes (24) and phagosomal pH (25) because effective proteolysis determines the fate of antigens, influencing antigen processing and presentation, which determines whether an efficient adaptive immune response is generated. As such, the elevated proteolysis that observed in this study in MDMs of APF+ individuals could induce stronger adaptive immune responses, which in turn, could promote robust inflammation, resulting in more severe host tissue damage and repair.

Chronic infection leads to inflammation and the production of inflammatory mediators that are toxic to invading pathogens (25). In the case of helminth infection, the helminthes could modulate host immune responses and switch immune responses from proinflammatory (Th1) to anti-inflammatory (Th2) responses (26). The key innate immune cells that play a significant role in this switching are MDMs, which can switch from M1- to M2-like phenotypes that can induce Th1 and Th2, respectively. Once recruited to chronic inflamed sites in response to local stimuli, M1 macrophages drive Th1 responses for pathogen clearance, whereas M2 macrophages drive Th2 responses for tissue remodeling and fibrosis (12). Therefore, in future studies, identification of MDM subsets from these populations of *O. viverrini* infected individuals will provide a better understanding of the mechanisms underlying the development of APF.

In conclusion, we measured and compared the phagocytic and proteolytic activities of MDMs between non-*O. viverrini*-infected control subjects, and *O. viverrini*-infected individuals with and without APF. [We also showed elevated ROS production in those with APF.](#) We propose that in the case of chronic *O. viverrini* infection, tissue resident macrophages with high phagocytic and proteolytic activities are the phenotypes that could damage bile duct epithelial and surrounding tissues, which results in the development of APF. Excessive production of

1
2
3
4
5
6
7
8
9
10
11
12
13
14
15
16
17
18
19
20
21
22
23
24
25
26
27
28
29
30
31
32
33
34
35
36
37
38
39
40
41
42
43
44
45
46
47
48
49
50
51
52
53
54
55
56
57
58
59
60

proinflammatory mediators from these macrophages might have effects on the parasites, but could also lead to excessive injury of surrounding tissue and hence result in extensive periductal fibrosis.

FUNDING

This work was supported by the Thailand Research Fund (TRF) grant number RTA 5680006, the Office of Higher Education Commission of Thailand - the Newton Fund Institutional Links - British Council, and partially from the National Institute of Allergy and Infectious Diseases (NIAID), NIH, grant number P50AI098639. BS is a TRF Senior Research Scholar.

ACKNOWLEDGEMENTS

We would like to thank John T. Cathey for editing the manuscript via the Publication Clinic KKU, Thailand. The content is solely the responsibility of the authors and does not necessarily represent the official views of the TRF, NIAID, OHEC-Newton Fund, or the NIH or the funders.

AUTHOR CONTRIBUTION

Conceived and design experiments: KS BS. Performed the experiments: KS EM BS. Analysis and/or data interpretation: KS ST SS BS. Contributed reagents/materials/analysis/technical expertise tools: EM SS ST SWE BS. Wrote the paper: KS SS ST SWE BS.

CONFLICT OF INTERESTS STATEMENT

The authors declare no conflict of interests.

REFERENCES

1. Sripa B, Bethony JM, Sithithaworn P et al. Opisthorchiasis and *Opisthorchis*-associated cholangiocarcinoma in Thailand and Laos. *Acta Trop* 2011; 120 Suppl 1: S158-168.
2. Elkins DB, Mairiang E, Sithithaworn P et al. Cross-sectional patterns of hepatobiliary abnormalities and possible precursor conditions of cholangiocarcinoma associated with *Opisthorchis viverrini* infection in humans. *Am J Trop Med Hyg* 1996; 55: 295-301.
3. Mairiang E, Chaiyakum J, Chamadol N et al. Ultrasound screening for *Opisthorchis viverrini*-associated cholangiocarcinomas: experience in an endemic area. *Asian Pac J Cancer Prev* 2006; 7: 431-433.
4. Mairiang E, Elkins DB, Mairiang P et al. Relationship between intensity of *Opisthorchis viverrini* infection and hepatobiliary disease detected by ultrasonography. *J Gastroenterol Hepatol* 1992; 7: 17-21.
5. Mairiang E and Mairiang P. Clinical manifestation of opisthorchiasis and treatment. *Acta Trop* 2003; 88: 221-227.
6. Sripa B, Kaewkes S, Sithithaworn P et al. Liver fluke induces cholangiocarcinoma. *PLoS Med* 2007; 4: e201.
7. Wynn TA and Ramalingam TR. Mechanisms of fibrosis: therapeutic translation for fibrotic disease. *Nat Med* 2012; 18: 1028-1040.
8. Borthwick LA, Wynn TA and Fisher AJ. Cytokine mediated tissue fibrosis. *Biochim Biophys Acta* 2013; 1832: 1049-1060.

1
2
3
4 336 9. Sripa B, Brindley PJ, Mulvenna J et al. The tumorigenic liver fluke *Opisthorchis*
5
6 337 *viverrini*-multiple pathways to cancer. *Trends Parasitol* 2012; 28: 395-407.
7
8
9 338 10. Pinlaor S, Sripa B, Sithithaworn P and Yongvanit P. Hepatobiliary changes, antibody
10
11 339 response, and alteration of liver enzymes in hamsters re-infected with *Opisthorchis*
12
13 340 *viverrini*. *Exp Parasitol* 2004; 108: 32-39.
14
15
16 341 11. Sripa B, Thinkhamrop B, Mairiang E et al. Elevated plasma IL-6 associates with
17
18 342 increased risk of advanced fibrosis and cholangiocarcinoma in individuals infected
19
20 343 by *Opisthorchis viverrini*. *PLoS Negl Trop Dis* 2012; 6: e1654.
21
22
23 344 12. Murray PJ and Wynn TA. Protective and pathogenic functions of macrophage
24
25 345 subsets. *Nat Rev Immunol* 2011; 11: 723-737.
26
27
28 346 13. Weidenbusch M and Anders HJ. Tissue microenvironments define and get reinforced
29
30 347 by macrophage phenotypes in homeostasis or during inflammation, repair and
31
32 348 fibrosis. *J Innate Immun* 2012; 4: 463-477.
33
34
35 349 14. Mairiang E, Laha T, Bethony JM et al. Ultrasonography assessment of hepatobiliary
36
37 350 abnormalities in 3359 subjects with *Opisthorchis viverrini* infection in endemic
38
39 351 areas of Thailand. *Parasitol Int* 2012; 61: 208-211.
40
41
42 352 15. Sripa B, Mairiang E, Thinkhamrop B et al. Advanced periductal fibrosis from
43
44 353 infection with the carcinogenic human liver fluke *Opisthorchis viverrini* correlates
45
46 354 with elevated levels of interleukin-6. *Hepatology* 2009; 50: 1273-1281.
47
48
49 355 16. Menck K, Behme D, Pantke M et al. Isolation of human monocytes by double gradient
50
51 356 centrifugation and their differentiation to macrophages in teflon-coated cell culture
52
53 357 bags. *J Vis Exp* 2014: e51554.
54

- 1
2
3
4 358 17. Yates RM and Russell DG. Phagosome maturation proceeds independently of
5
6 359 stimulation of toll-like receptors 2 and 4. *Immunity* 2005; 23: 409-417.
7
8
9 360 18. Wongratanacheewin S, Good MF, Sithithaworn P and Haswell-Elkins MR. Molecular
10
11 361 analysis of T and B cell repertoires in mice immunized with *Opisthorchis viverrini*
12
13 362 antigens. *Int J Parasitol* 1991; 21: 719-721.
14
15
16 363 19. Saichua P, Yakovleva A, Kamamia C et al. Levels of 8-oxodG predict hepatobiliary
17
18 364 pathology in *Opisthorchis viverrini* endemic settings in Thailand. *PLoS Negl Trop Dis*
19
20 365 2015; 9: e0003949.
21
22
23 366 20. Stuart LM and Ezekowitz RA. Phagocytosis: elegant complexity. *Immunity* 2005; 22:
24
25 367 539-550.
26
27
28 368 21. Kawai T and Akira S. The role of pattern-recognition receptors in innate immunity:
29
30 369 update on Toll-like receptors. *Nat Immunol* 2010; 11: 373-384.
31
32
33 370 22. Duffield JS, Lupper M, Thannickal VJ and Wynn TA. Host responses in tissue repair
34
35 371 and fibrosis. *Annu Rev Pathol* 2013; 8: 241-276.
36
37 372 23. Bility MT and Sripa B. Chronic *Opisthorchis viverrini* infection and associated
38
39 373 hepatobiliary disease is associated with iron loaded M2-like macrophages. *Korean J*
40
41 374 *Parasitol* 2014; 52: 695-699.
42
43
44 375 24. Reiser J, Adair B and Reinheckel T. Specialized roles for cysteine cathepsins in health
45
46 376 and disease. *J Clin Invest* 2010; 120: 3421-3431.
47
48
49 377 25. Watts C. The endosome-lysosome pathway and information generation in the
50
51 378 immune system. *Biochim Biophys Acta* 2012; 1824: 14-21.
52
53
54
55
56
57
58
59
60

1
2
3
4
5
6
7
8
9
10
11
12
13
14
15
16
17
18
19
20
21
22
23
24
25
26
27
28
29
30
31
32
33
34
35
36
37
38
39
40
41
42
43
44
45
46
47
48
49
50
51
52
53
54
55
56
57
58
59
60

379 26. Salgame P, Yap GS and Gause WC. Effect of helminth-induced immunity on infections
380 with microbial pathogens. *Nat Immunol* 2013; 14: 1118-1126.

382

FIGURE LEGENDS

FIGURE 1 MDMs from individuals with *O. viverrini*-induced APF phagocytosed more beads.

Numbers of phagocytosed opsonized silica beads covalently coupled to Alexa Fluor 594 were manually counted after synchronized phagocytosis for 60 min with MDMs from healthy individuals (A), *O. viverrini*-infected individual with no APF (B) and *O. viverrini*-infected individual with APF (C). Average number of phagocytosed beads per cell was calculated by manual counts (D). The % of phagocytic cells was also calculated (E). Data represents mean \pm SEM analyzed using the *t* test. * indicates a *p* value of <0.05 , and mean values are of at least 20 individual cells (chosen blinded) for each of the 102 samples in each cohort.

FIGURE 2 Proteolysis of MDMs from individuals with *O. viverrini*-induced with and without APF and healthy controls. Live MDMs that had undergone synchronized phagocytosis of silica beads covalently coupled with DQ-BODIPY BSA were continuously monitored for 60 min using an inverted live cell BioStation IM microscope. Representative images are shown in Figures A-C. Upper panels are bright-field images while lower panels are fluorescence images. The time course of proteolytic activity within the phagosome, measured as gain of fluorescence, is shown in Figure D. Data are mean \pm SEM analyzed using two-way repeated-measures ANOVA of 10-15 individual beads measured in each of the 102 samples in each cohort. * indicates a *p* value of <0.05

1
2
3
4
5
6
7
8
9
10
11
12
13
14
15
16
17
18
19
20
21
22
23
24
25
26
27
28
29
30
31
32
33
34
35
36
37
38
39
40
41
42
43
44
45
46
47
48
49
50
51
52
53
54
55
56
57
58
59
60

Figure 3 ROS production of monocytes in whole blood

Whole blood from healthy controls (OV-) or OV-infected individuals without (OV+/APF-) or with advanced periductal fibrosis (OV+/APF+) were incubated in the absence (unprimed) or presence of 5 ng/mL GM-CSF for 30 min. DHR 123 (at 5 μ M) was then added and then primed or unprimed cells were incubated with or without fMet-Leu-Phe for 5 min before analysis by flow cytometry and gating of monocyte responses. Figure 3A-C show mean fluorescent intensities of DHR123 from OV-, OV+/APF-, OV+/APF+ respectively. Figure 3D, () shows fMet-I-Phe responses in unprimed cells, () GM-CSF responses in the absence of fMet-Leu-Phe and () ROS production by fMet-Leu-Phe in GM-CSF cells. N = 51 per group for GM-CSF primed responses. Data represents mean \pm SEM analyzed using the *t* test. * indicates a p value of <0.05.

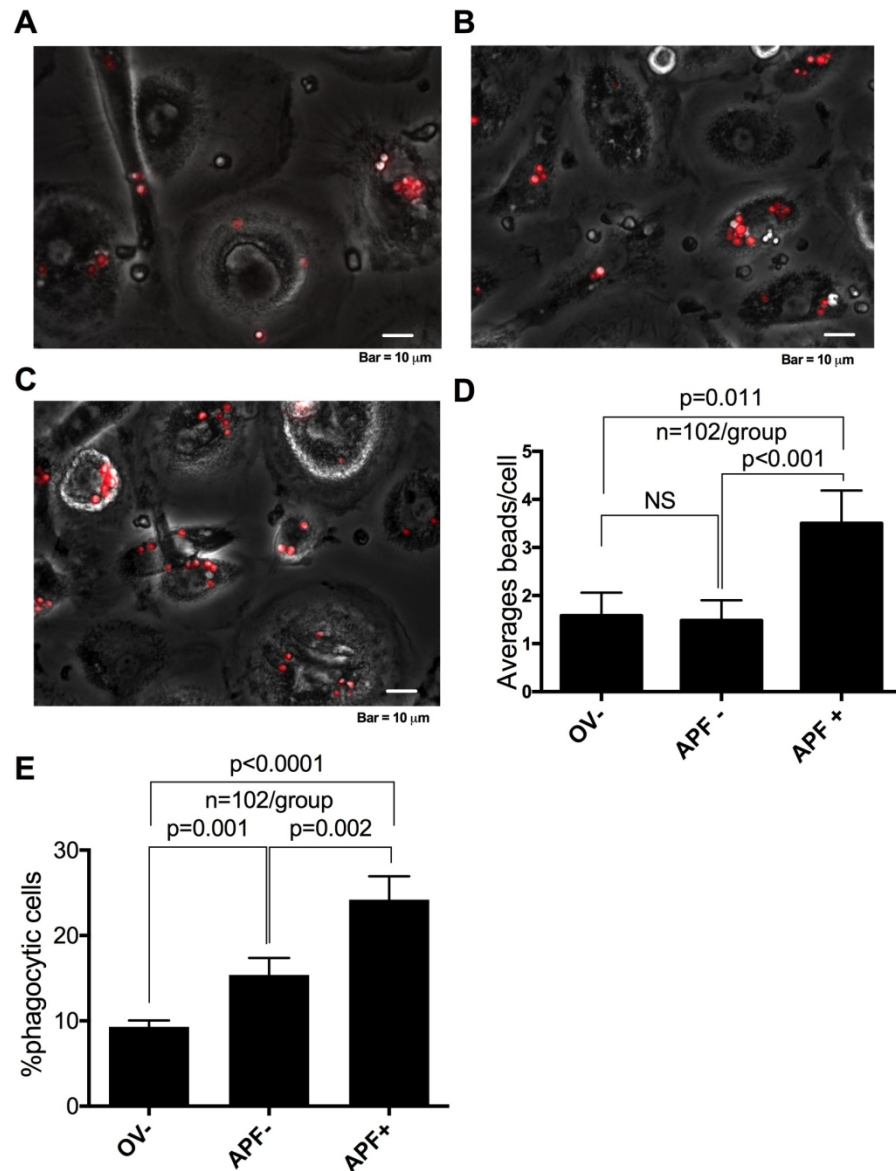


FIGURE 1 MDMs from individuals with *O. viverrini*-induced APF phagocytosed more beads. Numbers of phagocytosed opsonized silica beads covalently coupled to Alexa Fluor 594 were manually counted after synchronized phagocytosis for 60 min with MDMs from healthy individuals (A), *O. viverrini*-infected individual with no APF (B) and *O. viverrini*-infected individual with APF (C). Average number of phagocytosed beads per cell was calculated by manual counts (D). The % of phagocytic cells was also calculated (E). Data represents mean \pm SEM analyzed using the t test. * indicates a p value of <0.05, and mean values are of at least 20 individual cells (chosen blinded) for each of the 102 samples in each cohort.

142x185mm (300 x 300 DPI)

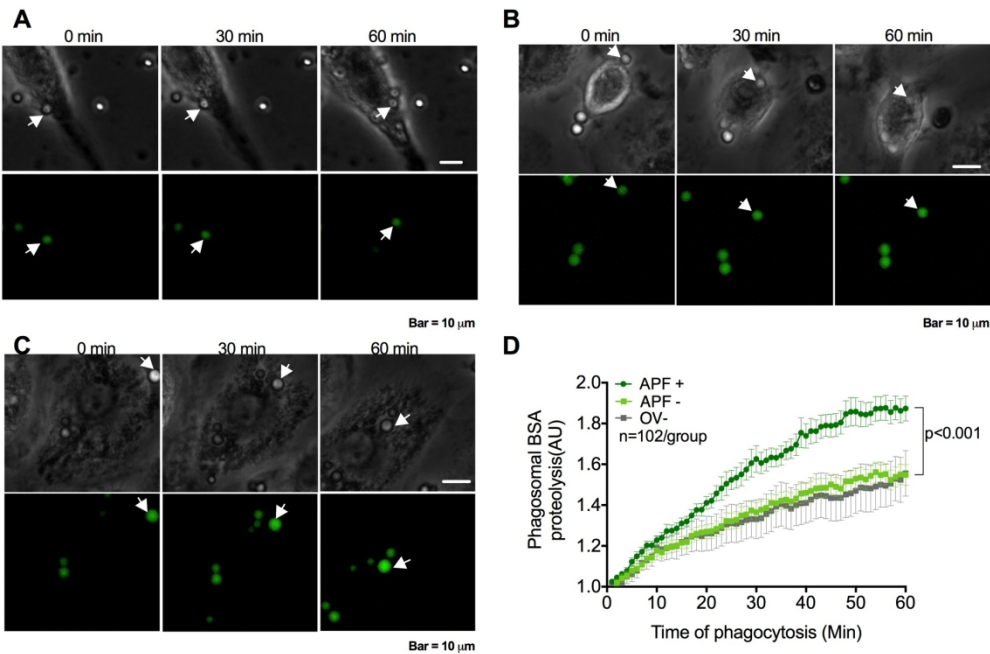


FIGURE 2 Proteolysis of MDMs from individuals with *O. viverrini*-induced with and without APF and healthy controls. Live MDMs that had undergone synchronized phagocytosis of silica beads covalently coupled with DQ-BODIPY BSA were continuously monitored for 60 min using an inverted live cell BioStation IM microscope. Representative images are shown in Figures A-C. Upper panels are bright-field images while lower panels are fluorescence images. The time course of proteolytic activity within the phagosome, measured as gain of fluorescence, is shown in Figure D. Data are mean \pm SEM analyzed using two-way repeated-measures ANOVA of 10-15 individual beads measured in each of the 102 samples in each cohort. * indicates a p value of <0.05

168x113mm (300 x 300 DPI)

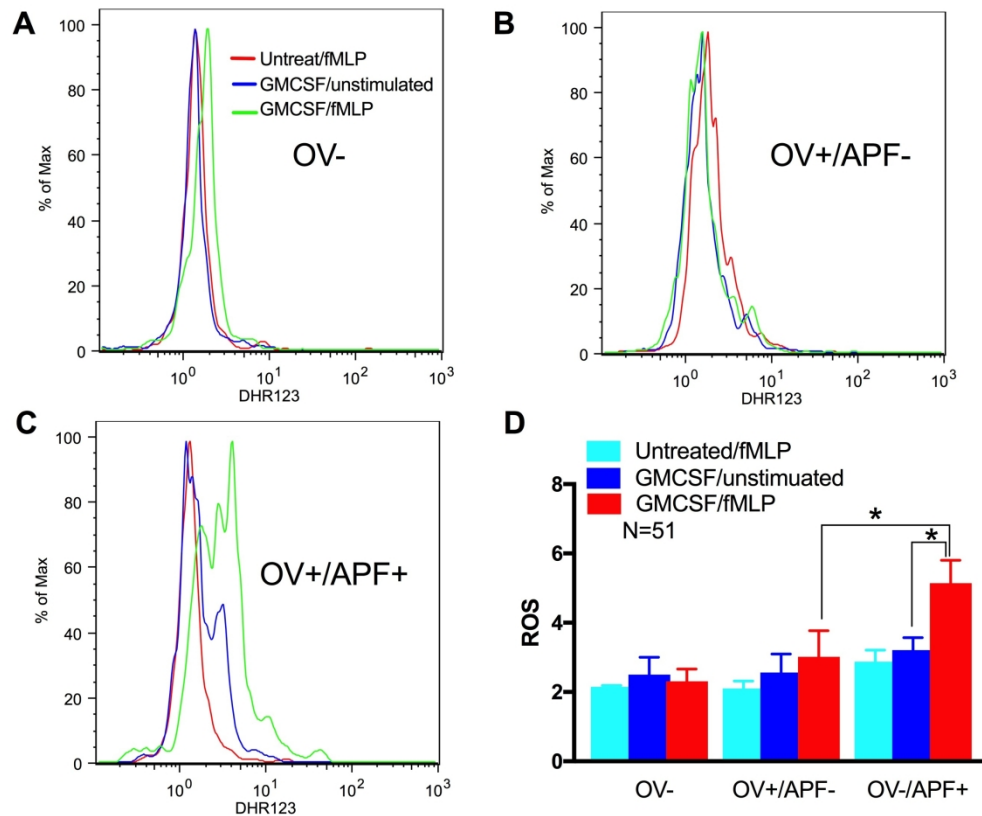


Figure 3 ROS production of monocytes in whole blood

Whole blood from healthy controls (OV-) or OV-infected individuals without (OV+/APF-) or with advanced periductal fibrosis (OV+/APF+) were incubated in the absence (unprimed) or presence of 5 ng/mL GM-CSF for 30 min. DHR 123 (at 5 μ M) was then added and then primed or unprimed cells were incubated with or without fMet-Leu-Phe for 5 min before analysis by flow cytometry and gating of monocyte responses. Figure 3A-C show mean fluorescent intensities of DHR123 from OV-, OV+/APF-, OV+/APF+ respectively. Figure 3D, () shows fMet-Leu-Phe responses in unprimed cells, () GM-CSF responses in the absence of fMet-Leu-Phe and () ROS production by fMet-Leu-Phe in GM-CSF cells. N = 51 per group for GM-CSF primed responses. Data represents mean \pm SEM analyzed using the t test. * indicates a p value of <0.05.

225x186mm (300 x 300 DPI)

Response to reviewers' comments

Reviewer: 1

Comments to the Author

Review on “Association between macrophages phagocytosis activities and advanced periductal fibrosis in chronic opisthorchiasis”

The presented manuscript analyses in vitro generated macrophages (MDM) from patients infected with *O.viverrini* exhibiting (APF+) or free from (APF-) signs of advanced periductal fibrosis. The authors report an enhanced uptake of opsonised silica beads by MDM from APF+ patients. The study seems for the most part technically sound and is well described. However the conclusions drawn seem rather speculative and are only loosely based on the presented data. Overall the extent of the presented findings is very limited and would need further experimental work to corroborate the authors claims.

Response: Thank you for your comments! We agree that the work presented in the previous submission was limited as only phagocytotic and proteolytic assays were included. We have therefore performed more experiments to support our claims and conclusions. We have now measured and compared ROS among these three groups. The results can be found from lines 230-245 and Figure 3.

Individual comments:

The conclusions drawn by the authors seem speculative and one-sided. Phagocytosis per se is not pro-inflammatory but can be anti-inflammatory and prevent chronic inflammation (e.g. phagocytosis of apoptotic cells during cystic fibrosis). Thus, the authors would need to include further data on cytokine production or other inflammatory mediators to clarify whether the enhanced rate of phagocytosis promotes or protects from APF.

Furthermore, the authors repeatedly imply that the altered phagocytosis rate observed in macrophages from APF+ patients may be causative for the formation of fibrosis. However, this is not supported by the presented data. Indeed, since none of the APF- patients (some of whom will develop APF eventually) show altered macrophage phagocytosis it would seem this is a consequence rather than a cause of fibrosis.

Response: In order to address this, we have now performed ROS assays. We found that ROS production by blood monocytes was higher in individuals with APF compared with healthy controls and infected individuals without APF. ROS is a key inflammatory mediator that could cause tissue damage if overexpressed. We believe that elevated ROS production can therefore contribute to tissue damage and promote persistent inflammation. Also, we have re-examined the phagocytosis data and have measured the % of monocytes that underwent phagocytosis (new Figure 1E). This new figure shows that in infected individuals without APF, a greater % of the population of macrophages were capable of phagocytosis, compared to non-infected controls. Therefore, infection *per se* leads to a great phagocytic activity of these macrophages.

The data presented in figure 3 is inconclusive and does not reflect on the rate of proteolysis in MDM. If I understand the experimental procedure correctly macrophages were incubated with BSA-Bodipy coupled silica beads and the release of Bodipy measured over time. However, the authors have already shown that MDM from APF+ patients take up more beads in a similar assay. Thus, the increased fluorescent signal might not reflect an altered rate of proteolysis but rather a higher uptake of substrate by the APF+ MDM. Therefore this data cannot be interpreted beyond what has already been shown in figure 1&2 and should be removed. Alternatively the authors would need to provide evidence of substrate normalisation.

Response: This is a very good point raised by the referee but unfortunately, we did not adequately explain the experiment or how the data were obtained. In fact, we actually measured the increase in fluorescence of individual ingested beads. We tracked the release of bodiopy from individual engulfed beads over the first 60 min of phagocytosis, measuring the fluorescence of 10-15 individual beads per patient sample (n= 102 patient samples). We apologise for not making the nature of this measurement clear in our first submission. We added a clearer explanation in the manuscript in line 218-220.

The flowcytometry data presented in figure 2 and the microscopy pictures shown in figure 1 seem to contradict each other. Whereas the microscopy suggests virtually all macrophages do phagocytose opsonised silica beads only about 1% of cells do so according to the flow cytometry data. Is this due to variation in donors and the specific datasets chosen? If so it might be more prudent to chose more representative images / flow-plots.

Also, please include the flow cytometry data as % positive cells rather than or in addition to the MFI of the whole population.

Response: We agree with these comments. We believe that the phagocytic capacity of the cultured macrophages was grossly perturbed when we scraped them from the culture plates prior to flow cytometry, which explains their very low activity. Therefore, we have removed this figure from the revised manuscript as we believe that the data are not representative of the true phagocytic activity of these cells. The images of phagocytosis shown in Figure 1A-C are single images but we have quantified the number of ingested particles and (new Figure 1E) the number of cultured macrophages (expressed as a % of the total number), that could undergo phagocytosis. We analysed at least 100 cells/patient and believe that these are a truer representation of the phagocytic capacity of these cells.

Since the authors use autologous serum to generate MDMs in vitro they should include data on the differentiation and activation status (i.e. MHC-expression, costimulatory molecules etc.) of the macrophages from the three groups. Does serum from APF+ patients induce altered differentiation / pre-activation of MDM?

Response: These are extremely helpful comments, but we now cannot do this retrospectively. We will include such measurements in a new study.

Thank you for your invaluable comments.

Reviewer: 2

Comments to the Author
The manuscript entitled "Association between macrophages phagocytosis activities and advanced periductal fibrosis in chronic opisthorchiasis" addresses a major gap in the knowledge on the pathogenesis of chronic opisthorchiasis, namely the role innate immune cells such as macrophages. The authors demonstrate that elevated macrophage phagocytic and proteolytic activities are associated with chronic OV-induced liver fibrosis. This study will establish the basis for more mechanistic studies on the role of macrophages in OV-induced liver disease.

Response: Thank you for your comments!